

Central Effects of Occipital Nerve Electrical Stimulation Studied by Functional Magnetic Resonance Imaging

Silvia Kovacs, MSc*, Ronald Peeters, PhD*, Dirk De Ridder, MD, PhD[†], Mark Plazier, MD[†], Tomas Menovsky, MD[†], Stefan Sunaert, MD, PhD*

Objective: To study the central effects of occipital nerve stimulation (ONS) using functional magnetic resonance imaging (fMRI).

Materials and Methods: After phantom measurements, blocked design fMRI scanning was performed during intermittent ONS in a healthy volunteer with implanted electrodes connected to an external generator. To assess the effect of frequency and stimulation mode, seven different frequencies in either tonic or burst mode were generated by a neurostimulator.

Results: A qualitative analysis of the main effect of ONS demonstrated significantly decreased activity within the bilateral primary visual, auditory, and somatosensory cortices and in the amygdala. Significant increased activity was observed bilaterally in the thalamus, frontal, and parietal areas and the cerebellum. Subsequently, quantitative analysis revealed that, unlike tonic mode stimulation, burst mode stimulation appeared to be frequency-dependent.

Conclusions: This study demonstrates the feasibility and safety of fMRI studies with simultaneous ONS in a subject with externalized electrodes. The activation and deactivation pattern induced by ONS depends on stimulation mode and frequency.

Keywords: chronic pain, implantation, magnetic resonance imaging, occipital nerve stimulation, safety

Conflict of Interest: Dr. DeRidder received an educational grant from St. Jude Medical. The other authors reported no conflicts of interest.

INTRODUCTION

Nowadays, there is an increasing interest in the use of electrostimulation in the neurosurgical treatment of patients suffering from various medically intractable diseases. Different neurostimulation techniques have been used in the treatment of pain, targeting parts of the central nervous system, such as the spinal cord, motor cortex, thalamus, periaqueductal gray (PAG), and hypothalamus (1–4). The peripheral nervous system has also been a focus of pain treatments using electrical stimulation, such as the infra- and supraorbital nerves and the greater and/or lesser occipital nerves (5–7). Occipital nerve stimulation (ONS) has proven effective for the treatment of patients with cervicogenic headache syndromes such as occipital neuralgia, and patients with occipital headache syndromes such as transformed migraine (6–8). Despite the upcoming use of different types of neurostimulation, the working mechanism of this kind of neurosurgical treatment remains largely unknown.

In this study we will focus on the working mechanism of subcutaneous ONS, which employs stimulation of the greater and/or lesser occipital nerves. As these nerves do not directly connect with structures within the cortex itself, it was thought that this kind of stimulation cannot bring about direct central effects. However, the occipital nerves interconnect with other nerves, in particular, the ophthalmic division of the trigeminal nerve (9), and form a continuous neural network affecting the trigeminal nucleus caudalis and the cervical dorsal horn at the C1 and C2 levels, which are collectively called the “trigemincervical complex” (8–13). One way to

study possible central effects is functional magnetic resonance imaging (fMRI).

Functional magnetic resonance imaging is a noninvasive technique that uses local changes in the concentrations of oxy- and deoxyhemoglobin to identify regions of altered neural activity (14) and has the potential to address several of the questions regarding this possible central mechanism. However, few fMRI studies evaluating the mechanism of neurostimulation have been conducted because of potential severe safety issues. Voltages and currents in neurostimulator leads induced by pulsed gradient magnetic fields and/or pulsed radiofrequency (RF) fields may result in harmful effects (15,16). Heating of the neurostimulator leads, which is due to the electromagnetic field, can also result in serious burn injuries

Address correspondence to: Stefan Sunaert, MD, PhD, University Hospitals Leuven, UZ Gasthuisberg, Department of Radiology, Herestraat 49, 3000 Leuven, Belgium. Email: stefan.sunaert@uzleuven.be

* University Hospitals Leuven, Department of Radiology, Herestraat 49, 3000 Leuven, Belgium; and

[†] University Hospital Antwerp, BRAI²N & Department of Neurosurgery, Wilrijkstraat 10, 2650 Edegem, Belgium

Source of financial support: This study was supported by grant G.0354.06 from the “Fund for Scientific Research-Flanders” FWO.

For more information on author guidelines, an explanation of our peer review process, and conflict of interest informed consent policies, please go to <http://www.wiley.com/bw/submit.asp?ref=1094-7159&site=1>

(17). Moreover, fMRI is also prone to artifacts resulting from the metallic components of neurostimulation systems (18). However, by means of severe safety precautions, such as phantom measurements that control for the induced heating and induced biologically harmful currents, inspection of wires for fraying, prevention of their contact with the patient, electronic control of overstimulation, and imaging sequences with low specific absorption rate (SAR), it might be possible to safely conduct the experiments.

To our knowledge, there has been no fMRI study at 3T testing the effects of ONS upon the central nervous system, nor any fMRI experiments visualizing the central effects of electrostimulation on healthy volunteers. The aim of the present study was twofold. On one hand, we wanted to demonstrate the feasibility and safety of using fMRI at 3T with simultaneous ONS. On the other hand, we wanted to assess the central fMRI activation patterns in a healthy volunteer both quantitatively and qualitatively. Moreover, we wanted to study possible effects because of different stimulation modes (burst and tonic) and to different frequencies. Understanding of these activation patterns may contribute to revealing the therapeutic mechanisms of ONS.

MATERIALS AND METHODS

Safety testing

In a phantom pilot study, voltage induced by the gradient fields, the RF fields, and the stimulator was measured by means of an analogue oscilloscope (LA314; LeCroy, Chestnut Ridge, New York, NY, USA; four channels; bandwidth = 400 MHz) for the different MRI sequences used in this study. To detect possible signal loss, the signal-to-noise ratio (SNR) was measured in both a gradient-echo echo-planar-imaging (GE-EPI) reference scan and the images acquired when the stimulator was switched on and off.

Subject

The study was approved by the institutional ethical committee and was conducted in accordance with the Convention of Helsinki. Informed consent was obtained from the 39-year-old right-handed healthy man subject without any history of neurologic disorders. The participant was implanted with two subcutaneous eight-contact electrodes (Octrode, St. Jude Medical, Plano, TX, USA) via a midline approach as depicted in Figure 1 (19). Under local xylocaine anesthesia, with the volunteer in prone position, a 2-cm straight sagittal incision was made 1 cm cranial of the occipital protuberance. A 14-gauge Touhy needle was inserted subcutaneously in the direction of the pinna of the ear. After removal of the stilet, the leads were inserted through the needle and the needle was then removed. The electrodes were anchored to the aponeurosis and the subcutis. Subsequently, the skin was closed. The electrodes were sutured tight to the skin.

An eight-channel digital neurostimulator (DS8000, World Precision Instruments, Sarasota, FL, USA), capable of delivering tonic and burst mode stimulation, was located outside the magnet room and connected to the external leads using a double-shielded twisted pair cable to avoid pick-up of RF-radiation. Furthermore, to avoid image artifacts, RF filters were placed which provide reduced signals from certain (not described here) frequency bands. Prior to scanning, the subject was asked to subjectively determine the strength and location of stimulation to be equal at both sides of his head. This resulted in a stimulation strength of 1.0 and 2.5 V for the right and left side, respectively. The leads were disconnected when placing

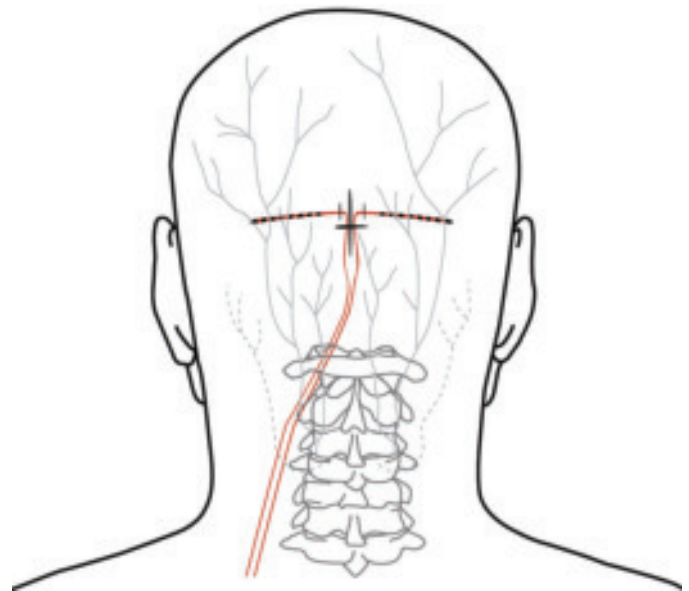


Figure 1. Schematic of the lead positioning in the subcutaneous occipital area. Schematic of the midline subcutaneous approach in lead positioning for electrical stimulation of the occipital nerves.

the subject into the magnet, and only connected to the external stimulator when the patient's head was positioned in the center of the magnet.

Data acquisition

Functional magnetic resonance imaging scanning was performed on a 3T MR system (Achieva, Philips, Best, the Netherlands) with a transmit body RF coil and a receive-only RF head coil configuration using a T2*w single shot GE-EPI sequence (35 contiguous transverse slices of 4 mm thickness, TR/TE = 3000/33 msec, acquired voxel size = $2.88 \times 2.88 \times 4.00 \text{ mm}^3$, reconstructed voxel size = $1.8 \times 1.8 \times 4.0 \text{ mm}^3$, FOV = $230 \times 230 \text{ mm}^2$, reconstructed matrix = $128 \times 128 \text{ mm}^2$, SENSE-reduction factor = 2, flip angle = 90°). Using this sequence, low SAR values (whole body < 0.0 W/kg and head = 0.7 W/kg) were obtained. Additionally, a high-resolution anatomic dataset (3D TFE) for overlay on the functional datasets with following scan parameters was acquired: 230 contiguous coronal slices of 1-mm thickness, TR/TE = 9.74/4.6 msec, reconstructed voxel size = $0.49 \times 0.49 \times 1.00 \text{ mm}^3$, FOV = $250 \times 180 \text{ mm}^2$, reconstructed matrix = $512 \times 512 \text{ mm}$, flip angle = 8° . The SAR values for this sequence were even lower, that is <0.0 W/kg (whole body) and =0.2 W/kg (head).

The stimulation paradigm consisted of a block design which included six off/on periods of ten scans each. During the on periods, the stimulator generated seven different stimulation frequencies empirically chosen within the physiologic frequency range. Frequencies were either harmonics of 3 Hz (3, 6, 12, and 18 Hz) or harmonics of 5 Hz (5, 10, and 20 Hz) and were presented either in tonic mode (one spike) or burst mode (eight spikes at 500 Hz). During the off periods, no electrical pulses were generated. In total, there were 14 runs of 120 dynamics each.

Data analysis

Data were analyzed off-line using SPM2 software (Statistical Parametric Mapping, Wellcome Department of Imaging Neuroscience,

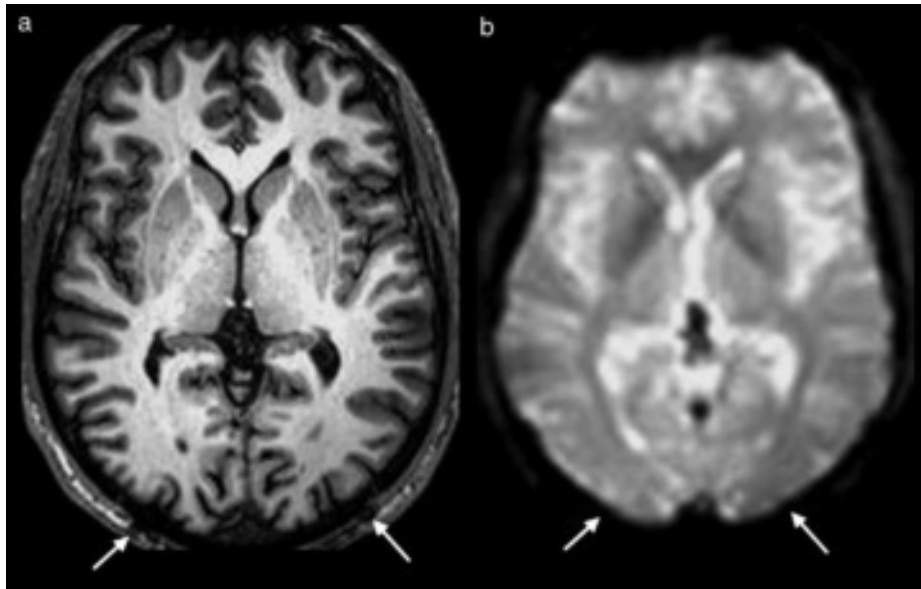


Figure 2. Electrode position and susceptibility artifacts. (a) An axial 3D TFE T1-weighted anatomic image visualizing the electrode position (white arrows). (b) An axial GE-EPI image without any noticeable susceptibility artifact near the electrodes (white arrows). GE-EPI, gradient-echo echo-planar-imaging.

University College London, London, UK). For each scan, the images were realigned, coregistered to the high-resolution T1w anatomic images, spatially normalized to the Montreal Neurological Institute standard brain, and spatially smoothed with a Gaussian kernel of FWHM = 5 mm. The images were then entered in a statistical analysis based on General Linear Model statistics which generated an individual statistical parametric map for following contrasts: “all stimulation vs. no stimulation,” “burst mode more than tonic mode,” and “tonic mode more than burst mode.” These contrasts were assessed in more detail for both qualitative and quantitative analysis.

For qualitative analysis, we used a significance threshold of $p < 0.05$ corrected for multiple comparisons. Anatomic labeling of significantly activated local maxima was performed using the automated anatomic labeling (AAL) map of Chris Rorden’s MRICro v1.40 (20) according to the methods described by Tzourio-Mazoyer et al. (21).

For quantitative analysis, spherical regions of interest (ROIs) of 27 voxels each were drawn around the local maxima extracted from the different contrasts described above. Percent MR-signal change of the 14 different time series was extracted in each ROI using an automated homebuilt procedure in SPM2. In order to investigate the effect of stimulation mode, a mean of the percent MR-signal change was calculated for seven time series taken together, performed with either burst or tonic stimulation. The obtained mean values for the percent MR-signal change of burst and tonic mode were compared using an unpaired two-tailed Student’s *t*-test. Significance threshold was set at $p < 0.05$. For the effect of frequency, the mean of the percent MR-signal change was calculated for each time series separately.

RESULTS

Safety testing and image quality

No (heating-related) complications of ONS were noted while performing fMRI, nor did the subject report any RF-induced electrophysiologic effects such as paresthesia.

In accordance with the measurement of Georgi et al. (16), no induced voltage could be demonstrated on the oscilloscope when switching on the gradient fields by reducing the flip angle to 0° . When switching on the RF fields, however, a modulated sinusoidal waveform with an amplitude up to 6 V and a carrier frequency of 128 MHz, according to the magnetic field strength of 3T, could be shown.

No image artifacts, such as susceptibility signal drop-outs near the electrical leads, were present in the datasets, nor was there evidence of contamination because of RF noise from outside the scanner room (Fig. 2). The measured SNR in EPI images acquired with the neurostimulator switched off and on was identical and similar to the reference scan prior to electrode implantation.

Main effect “all stimulation vs. no stimulation”

Figure 3 and Table 1 depict the location of significantly activated (stimulation more than baseline) and deactivated (baseline more than stimulation) foci obtained after analysis of the main effect “all stimulation (irrespective of frequency and mode) vs. no stimulation.” A large network of significantly activated foci was found (Table 1), which includes the hypothalami, the thalami, the orbito-frontal cortex, the premotor cortex, the PAG, the inferior parietal lobe, and the cerebellum. **In primary areas like the primary motor (M1), visual (V1), auditory (A1), and somatosensory area (S1), the activation is suppressed (deactivation). In addition, a deactivation of the paracentral lobule, secondary somatosensory area (S2), the amygdala, the hippocampus, and the supplementary motor area (SMA) is demonstrated.**

Effect of stimulation mode

In general, we observed that activation and deactivation were more pronounced when stimulating with tonic compared with burst mode. In Figure 4, the effect “burst vs. tonic mode” is visualized in 12 representative locations. In the globally activated foci (Fig. 4a–f), a significantly ($p < 0.05$) higher percent MR-signal change was

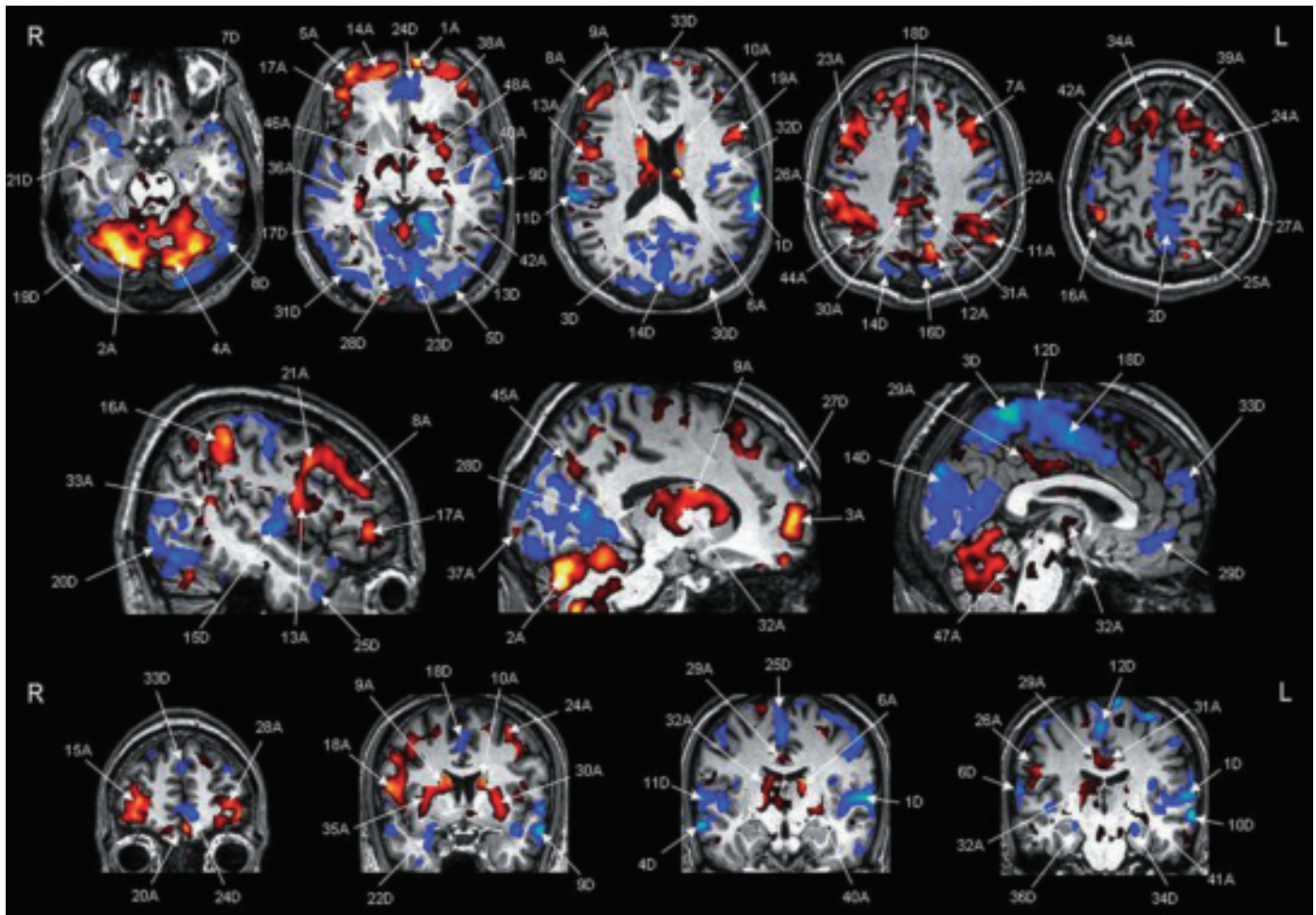


Figure 3. Main effect of “all stimulation vs. no stimulation” significantly activated (red) and deactivated (blue) foci ($p_{\text{corrected}} < 0.05$) obtained after analysis of the main effect “all stimulation vs. no stimulation,” overlaid on axial (above), sagittal (middle), and coronal (below) slices of a spatially normalized T1-weighted brain. Labeling is according to Table 1. L, left; R, right.

obtained when stimulation was performed in tonic mode compared with burst mode. This is demonstrated in the middle figure by a blue color. The opposite was true for the globally deactivated foci (Fig. 4g–k). Except for the right amygdala (Fig. 4l), these foci experience a larger deactivation change when stimulating in tonic mode, hence the red color in the middle figure.

Effect of stimulus frequency

Effects related to the used stimulation frequency were observed. In Figure 5, the mean percent MR-signal change of the seven different frequencies in either burst or tonic mode is plotted for the same 12 different locations depicted in Figure 4. In case of tonic stimulation mode, all frequencies seem to contribute in the same manner to the overall brain activity (activation or deactivation). Frequencies of 5, 6, 18, and 20 Hz provoke the largest changes, while 3, 10, and 12 Hz stimulation elicit only minor central nervous system activation. In case of burst stimulation mode, a dichotomous reaction seems to be present for multiples of 3 Hz (3, 6, 12, and 18 Hz) and 5 Hz (5, 10, and 20 Hz). Stimulation with multiples of 3 Hz induces more pronounced activations or deactivations in the brain compared with stimulating with multiples of 5 Hz. Moreover, there seems to be a slight intensity effect of 3, 6, and 18 Hz, with 3 Hz inducing the

smallest and 18 Hz the largest percent MR-signal change. Note that these frequency-related effects are different in the right amygdala (Fig. 4l). In case of burst mode stimulation, unlike tonic mode stimulation, all frequencies contribute in the same manner to the brain deactivation.

DISCUSSION

In this manuscript we demonstrated the feasibility of using fMRI at 3T with simultaneous ONS in a healthy volunteer. During ONS distinct (de)activation patterns could be visualized. The extent and magnitude of these (de)activations seem to be dependent upon the stimulation mode and frequencies used.

Safety

In general, fMRI is regarded as an extremely safe, noninvasive diagnostic technique (22). However, literature reports problematic safety issues and even patients' injuries when performing (functional) MRI with neurostimulation systems present (23–25). The two principal MR safety concerns for electrical stimulation devices include RF-induced heating and induced electrical currents (15–17,26–29).

Table 1. Main Effect "All Stimulation vs. No Stimulation."

Activations							Deactivations						
Label	Anatomic area	Side	MNI-coordinates			t-value	Label	Anatomic area	Side	MNI-coordinates			t-value
			x	y	z					x	y	z	
11A	Angular gyrus	L	-50	-60	48	10.88	35D*	Amygdala	R	20	-4	-14	-7.00
44A	Angular gyrus	R	44	-58	46	7.39	23D	Calcarine fissure	L	-8	-84	-6	-10.71
38A	Anterior cingulate gyrus	L	-6	26	-8	8.38	28D	Calcarine fissure	R	10	-86	-2	-9.56
37A	Calcarine	R	14	-104	-4	8.45	8D	Cerebellum (crus1)	L	-48	-50	-30	-12.93
10A	Caudate nucleus	L	-16	4	18	10.91	19D	Cerebellum (crus1)	R	46	-70	-18	-11.13
9A	Caudate nucleus	R	18	2	18	11.04	16D	Cuneus	L	-8	-90	36	-11.50
4A	Cerebellum	L	-14	-76	-22	12.45	14D	Cuneus	R	8	-86	38	-12.07
2A	Cerebellum	R	14	-76	-32	13.32	20D	Fusiform gyrus	R	46	-77	11	-11.05
20A	Gyrus rectus	L	-2	52	-16	10.36	34D	Hippocampus (anterior)	L	-24	-18	-16	-7.49
41A	Hippocampus (posterior)	L	-36	-32	-6	7.80	36D	Hippocampus (anterior)	R	22	-20	-12	-6.71
36A	Hippocampus (posterior)	R	30	-38	0	8.87	21D	Inferior frontal gyrus (pars orbitalis)	R	26	10	-22	-10.94
48A	Hypothalamus	L	-10	-10	-12	5.48	5D	Inferior occipital gyrus	L	-36	-94	-6	-13.42
46A	Hypothalamus	R	6	-8	-10	6.95	31D	Inferior occipital gyrus	R	38	-86	-6	-8.48
19A	Inferior frontal gyrus (pars opercularis)	L	-50	16	10	10.39	13D	Lingual gyrus	L	-10	-44	2	-12.12
18A	Inferior frontal gyrus (pars opercularis)	R	52	14	10	10.47	17D	Lingual gyrus	R	8	-44	-2	-11.31
17A	Inferior frontal gyrus (pars orbitalis)	R	44	44	-2	10.48	18D	Middle cingulate gyrus	R	4	-6	50	-11.21
8A	Inferior frontal gyrus (pars triangularis)	R	50	36	22	11.06	24D	Middle frontal gyrus (pars orbitalis)	L	-8	52	-6	-10.34
22A	Inferior parietal gyrus	L	-46	-48	48	10.02	29D	Middle frontal gyrus (pars orbitalis)	R	0	40	-10	-9.38
16A	Inferior parietal gyrus	R	48	-44	56	10.54	30D	Middle occipital gyrus	L	-36	-90	20	-9.24
31A	Middle cingulate gyrus	L	-6	-28	34	9.50	9D	Middle temporal gyrus	L	-66	-20	-4	-12.89
29A	Middle cingulate gyrus	R	6	-40	46	9.55	6D	Middle temporal gyrus	R	68	-30	2	-13.18
28A	Middle frontal gyrus	L	-36	52	2	9.68	4D	Middle temporal gyrus	R	62	-12	-14	-13.82
15A	Middle frontal gyrus	R	32	52	4	10.61	26D	Middle temporal gyrus (temporal pole)	R	46	14	-38	-10.26
7A	Middle frontal gyrus	L	-40	20	46	11.14	2D	Paracentral lobule	L	-2	-40	64	-14.31
23A	Middle frontal gyrus	R	48	10	40	10.02	12D	Paracentral lobule	L	2	-26	74	-12.12
24A	Middle frontal gyrus	L	-34	6	58	9.99	3D	Precuneus	R	2	-44	66	-14.05
42A	Middle frontal gyrus	R	38	10	58	7.74	32D	Rolandic operculum	L	-34	-18	18	-8.40
1A	Middle frontal gyrus (pars orbitalis)	L	-10	66	-4	13.42	27D	Superior frontal gyrus	R	14	60	32	-9.64
5A	Middle frontal gyrus (pars orbitalis)	R	38	56	-6	12.00	33D	Superior frontal gyrus (pars medialis)	R	4	62	26	-8.25
33A	Middle temporal gyrus	R	48	-50	16	9.11	10D	Superior temporal gyrus	L	-54	-28	8	-12.30
40A	Pallidum	L	-24	-12	0	8.01	15D	Superior temporal gyrus	R	50	-8	4	-11.76
43A*	Periaqueductal gray	L	-6	-28	-8	7.70	1D	Superior temporal gyrus	L	-68	-28	20	-16.03
47A	Periaqueductal gray	R	4	-26	-8	6.86	11D	Superior temporal gyrus	R	60	-30	20	-12.14
27A	Postcentral gyrus	L	-52	-38	58	9.80	7D	Superior temporal gyrus (temporal pole)	L	-40	18	-28	-13.03
21A	Precentral gyrus	R	46	8	38	10.26	22D	Superior temporal gyrus (temporal pole)	R	28	6	-26	-10.86
12A	Precuneus	L	-12	-66	42	10.85	25D	Supplementary motor area	R	4	-18	60	-10.33
45A	Precuneus	R	16	-66	30	7.19							
30A	Putamen	L	-26	6	0	9.50							
35A	Putamen	R	24	2	12	8.95							
13A	Rolandic operculum	R	50	2	14	10.83							
34A	Superior frontal gyrus	R	10	28	58	8.96							
39A	Superior frontal gyrus (pars medialis)	L	-12	30	60	8.31							
3A	Superior frontal gyrus (pars medialis)	R	10	62	6	12.75							
14A	Superior frontal gyrus (pars orbitalis)	R	22	56	-2	10.76							
25A	Superior parietal gyrus	L	-18	-62	54	9.89							
26A	Supramarginal gyrus	R	58	-28	40	9.86							
6A	Thalamus	L	-12	-12	20	11.74							
32A	Thalamus	R	10	-4	10	9.49							

*Not shown in Figure 3.

Anatomic location, MNI-coordinates, and t-value for local maxima of significant (de)activation ($p < 0.05$) extracted from the contrast "all stimulation vs. no stimulation." L, left; R, right.

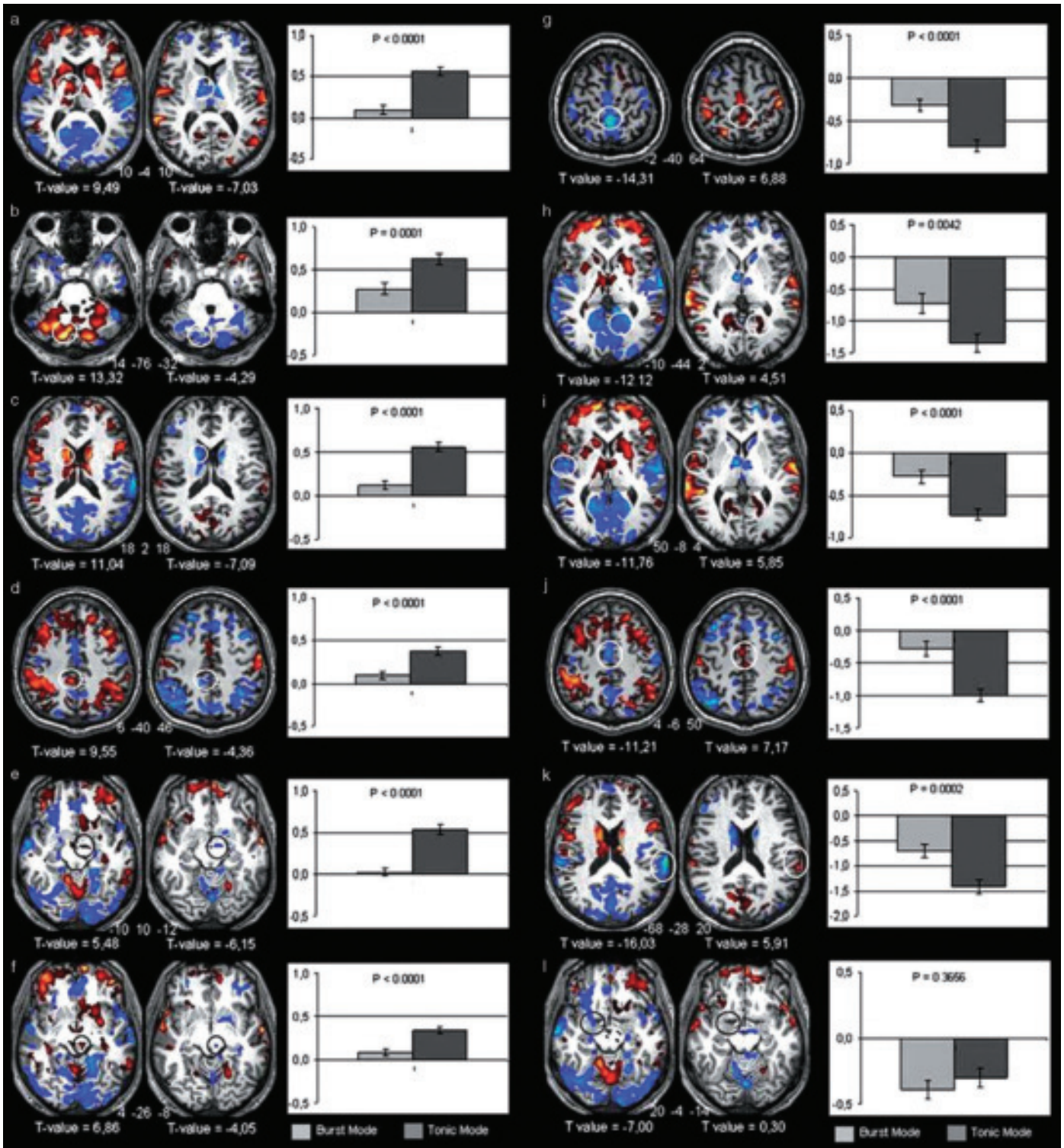


Figure 4. Effects of stimulation mode. The effect “burst vs. tonic mode” visualized in 12 locations (a–l). These are the right thalamus (a), the right cerebellum (b), the right caudate nucleus (c), the right middle cingulate gyrus (d), the left hypothalamus (e), the right periaqueductal gray (PAG) (f), the left paracentral lobule (S1) (g), the left lingual gyrus (V1) (h), the right transverse temporal gyrus (A1) (i), the right anterior cingulate gyrus (j), the left superior temporal gyrus (S2) (k), and the right amygdala (l). For each location, the left picture shows the general effect of “all stimulation vs. no stimulation,” overlaid on axial slices of a spatially normalized T1-weighted brain. Significantly activated foci are shown in red and significantly deactivated foci are colored blue ($p_{corrected} < 0.05$). Foci of interest (in MNI-coordinates) are indicated by circles with corresponding t -values printed below. In the middle picture the significantly activated foci obtained after analysis of the effects “burst mode more than tonic mode” and “tonic mode more than burst mode” are overlaid on a spatially normalized T1-weighted brain and depicted in red and blue, respectively ($p_{corrected} < 0.05$). Foci of interest are again indicated by circles with corresponding t -values printed below. In the right graph the mean percent MR-signal change \pm SEM after stimulation in burst and tonic mode is plotted for the marked foci. Plotted p -values were obtained after an unpaired t -test to verify the significance ($p < 0.05$) between the two bar graphs. MR, magnetic resonance.

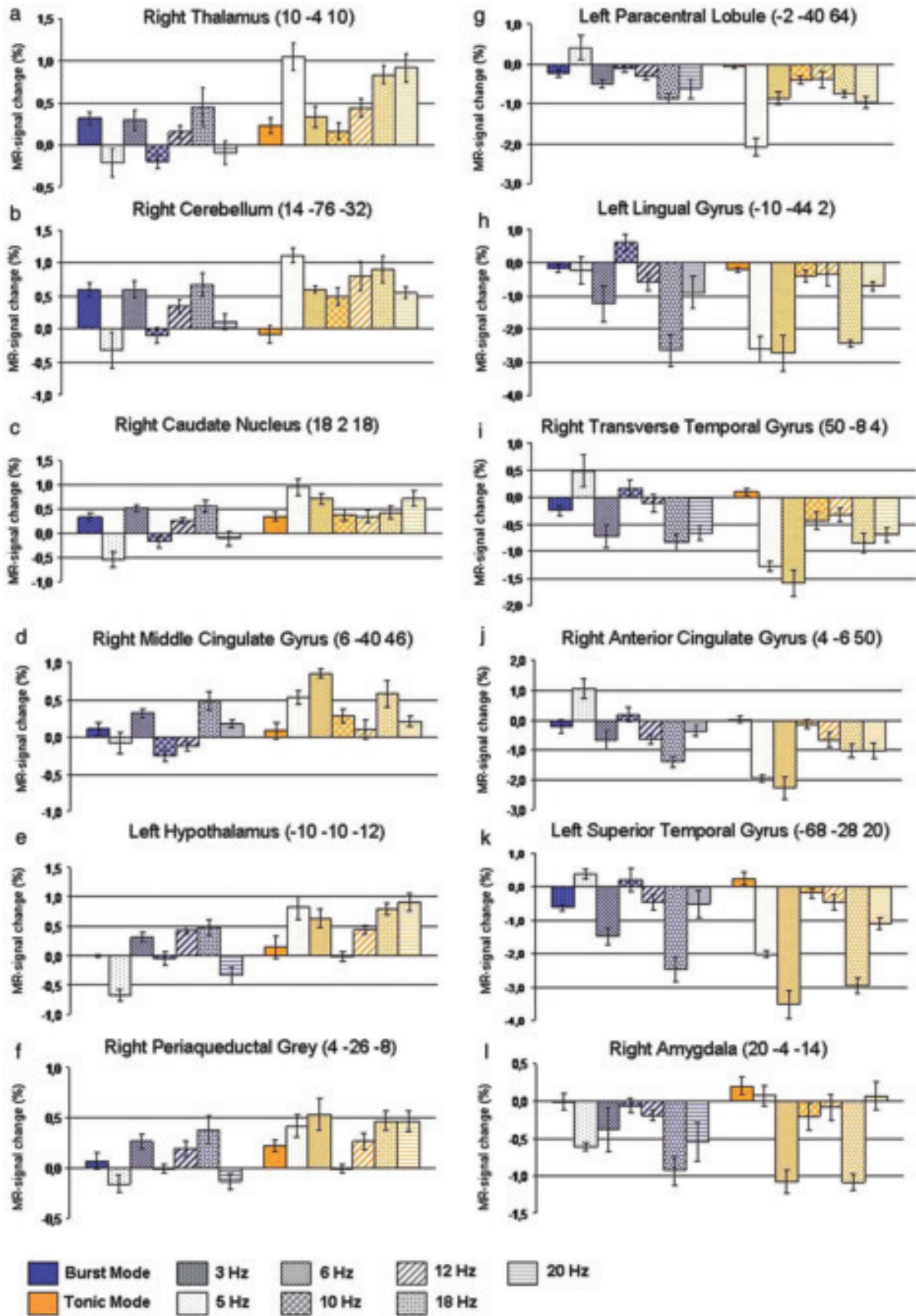


Figure 5. Effects of different frequencies at different stimulation modes. Bar graphs of mean percent MR-signal change \pm SEM during stimulation in burst (blue) and tonic (orange) mode plotted for seven different stimulation frequencies (3, 5, 6, 10, 12, 18, and 20 Hz) in six activated locations (a–f) and six deactivated locations (g–l). Different frequencies are indicated by different patterns. MR, magnetic resonance.

Radiofrequency-Induced Heating

Radiofrequency-induced heating that can occur because of absorption of RF energy by the tissue is an important safety issue as a temperature increase of $>5^{\circ}\text{C}$ at the electrodes or their leads causes a reversible malfunction of the neurons (30). A temperature of $>50^{\circ}\text{C}$ results in severe irreparable coagulation of brain matter or subcutaneous tissue (31). Routinely, SAR has been used as an indirect quantitative measure of RF energy in safety recommendations for clinical MRI procedures when conductive implants are present (17,22,29). Literature (17,26) states that it is imperative to use sequences with local SARs below 2.4 W/kg (whole-body averaged SAR smaller than 0.09 W/kg). However, other aspects resulting in RF-induced heating have to be taken into account: the position of the electrical leads (including the position in the patient and the relative position within the magnet), the used RF coils, the level of RF power, and hence the used sequences (15,16).

Georgi et al. (16) studied the effect of lead position on temperature elevation. When the lead was connected and placed along the z-axis of the scanner, no heating could be seen for low-SAR sequences such as GE-EPI. For high-SAR sequences such as T1w spin echo (SE), they measured heating directly at the electrode in the range of tenths of a degree Celsius. When the lead was placed closer to the RF coils (i.e., halfway between the scanner's z-axis and tunnel wall), the temperature increase directly at the electrode was significantly higher ($\pm 2^{\circ}\text{C}$), irrespective of type of sequence. The greatest effects associated with temperature increase were observed when the lead was placed along the scanner's tunnel wall, where the RF coils were located. That is an increase in temperature of 15.6°C at the electrode and 59.1°C along the lead outside the phantom, which was observed for the T1 SE sequence. For the GE-EPI sequence, the heating was 2.0°C and 3.4°C , respectively. Based on these observations, we have chosen to position our leads centrally in the magnet bore along the z-axis of the scanner.

Rezai et al. (17) and Finelli et al. (26) conducted *in vitro* MRI-related heating studies using a 1.5T MR system with bilateral deep brain stimulation systems positioned in a gel-filled phantom. They found clinically insignificant temperature elevations of $<2^{\circ}\text{C}$ in association with clinical sequences used for brain imaging. However, these results were obtained using a transmit-receive head RF coil, which minimizes the exposure of the leads/neurostimulation system to the MRI RF fields. Recently, Bhidayasiri et al. (15) measured, a temperature elevation of 2.1°C , despite the greater risk of using a transmit body RF-coil and receive-only head RF coil configuration. Based on previous studies of RF and other thermal ablation techniques, they concluded that transient temperature elevation of 2°C or less is unlikely to cause significant adverse thermogenic-related effects (32,33). Therefore, we used our standard transmit body RF-coil and receive-only head RF coil configuration to perform our measurements.

Induced Electrical Currents

Another important safety issue is the induction of voltage within the leads because of the presence of RF pulses and gradient fields. RF fields induce currents in electrical conductors that can result in an induced voltage and excessive heating. In addition, magnetic field gradients can induce currents in the electrodes that may result in neuronal stimulation (15).

In a previous feasibility study, Georgi et al. (16) measured the potential-induced voltages by means of an oscilloscope. They did not see any line surges induced by switching gradients, even with sequences that had particularly high slew rates such as GE-EPI. In contrast to the switching gradients, the RF pulses induced a significant voltage. For a GE-EPI sequence with the leads positioned along the z-axis of the scanner, the induced voltages had a maximum amplitude of about 7 V when the stimulator was switched on. The

frequency of the induced voltage was 64 MHz, which corresponds to the magnetic field strength of 1.5T. The amplitude of the induced voltage was much higher when the connecting lead was positioned along the RF coils of the scanner. The induced voltage when using a SE sequence had an even higher amplitude of more than 5 kV. They concluded that the amplitude of the induced voltage depends considerably on the image sequence and the position of the leads. However, based on other previous studies (34,35), they concluded that an alternating voltage with frequencies higher than 10 kHz does not evoke action potentials in neuronal cells, even if the amplitude is in a physiologic effective range of a few volts. In this setting, a neurophysiologically relevant, net averaged voltage of 0 V can be assumed as the biological system is too slow to respond to a fast decrease in voltage. Therefore, untriggered stimulation of neurons and artificial neuronal activations during fMRI examination are not expected.

In conclusion, ours and previous studies have indicated that MRI examinations are harmless, in subjects with externalized electrodes, if these safety precautions are taken into account. It should be noted, however, that in subjects with internalized electrodes additional safety concerns will emerge that make MRI examinations unwarranted. Furthermore, Baker et al. (29) showed that MR criteria defined using a particular MR system configuration may not be readily applied to another. Therefore, it is essential, before scanning a volunteer, that safety experiments are reproduced for each specific setup.

Image quality

Another concern related to performing MRI in the presence of conductive implants is the image quality. This can be affected in two ways. First, the electrodes and leads represent transitions in susceptibility and thus lead to signal loss because of $T2^*$ relaxation. This effect is an important factor in GE sequences, especially GE-EPI (16). However, by applying parallel imaging (SENSE-reduction factor = 2), there is no reduction in signal intensity visible near the implanted electrodes on the GE-EPI image in Figure 2b. Second, problems may arise from the pick-up of external RF sources by the connecting cable between the electrodes and the stimulator that is located outside the magnet room. To avoid image artifacts caused by RF power from external sources, RF filters were placed as electrical isolation. As depicted in Figure 2b, no characteristic pattern of straight lines along the frequency-encoding direction was seen in the GE-EPI image.

Central nervous system effects of occipital nerve stimulation

The second goal of this study was to visualize the central effects evoked by ONS in a healthy volunteer by means of fMRI. **Because of the absence of direct connections between the occipital nerves and with structures within the cortex itself, it was thought that stimulating these nerves cannot bring about central effects. However, our results show clear central nervous system effects of ONS. Areas of activation were predominantly seen in the hypothalamus, the thalamus, the orbitofrontal cortex, the prefrontal cortex, the PAG, the inferior parietal lobe, and the cerebellum. Deactivation was seen in primary areas (M1, V1, A1, and S1), the amygdala, the paracentral lobule, the hippocampus, S2, and SMA.**

Matharu et al. (36) have found central effects of ONS by means of a positron emission tomography (PET) study in patients with chronic migraine. There were significant changes in regional cerebral blood flow (rCBF) in brain areas associated with pain, such as cingulate cortex, insula, frontal cortex, thalamus, basal ganglia, and cerebellum.

A possible explanation for central effects induced by ONS is the various indirect connections from the occipital nerves to the cortex. First, the occipital nerves do have excitatory connections with other nerves, in particular, the ophthalmic division of the trigeminal nerve (8,9) and form a continuous neural network affecting the trigeminal nucleus caudalis and the cervical dorsal horn at the C1 and C2 levels, collectively called the trigeminocervical complex (10–13). The nucleus caudalis, located at the top of the spinal cord, projects to the thalamus which is a relay-station that distributes information to specific areas of the cortex. **Second, different (reciprocal) connections were found between C2 and the hypothalamus (37), the orbitofrontal cortex (38), the amygdala (37,38), the caudate nuclei (39), the PAG (40,41), the thalamus (40,42), and the cerebellum (43).**

Based on our main results ((de)activation irrespective of type of stimulation mode and frequency), and the above described (indirect) connections, one might suggest a possible working mechanism of ONS for pain treatment, in which the thalamus may play a key role. ONS led to activation of the thalamus in our study. In addition, literature has shown that the thalamus, especially the nucleus reticularis, functions as an inhibitory gate which can regulate the patterns of sensory input from the thalamus to the cortex (44). Although the resolution of our present fMRI technique is inadequate to parcelate different nuclei of the thalamus, our thalamic activity is seen at the outer rim of the thalamus (Fig. 3), and might thus correspond to the nucleus reticularis. Subsequently, the deactivation of the primary somatosensory (S1), auditory (A1) and visual (V1) cortices, the amygdala, the secondary somatosensory cortex (S2), and SMA may be a result of the inhibitory effect of the nucleus reticularis. Furthermore, it has been shown that in patients with peripheral neuropathic pain, there is a relative hypoperfusion of the thalamus (45). **Additionally, in functional imaging studies on pain, different regions of the “pain-matrix” such as S1, S2, and the amygdala are generally activated (46). Therefore, ONS might reactivate the thalamus in chronic neuropathic pain diseases like occipital neuralgia and subsequently suppress the hyperactive S1, S2, and amygdala.**

It should be noted, however, that this is a suggestive, not verified hypothesis and further research of the central working mechanism of ONS is crucial to compare results in both patients with chronic headache syndromes such as neuralgia and healthy volunteers. **However, in previous PET studies with motor cortex stimulation (MCS) for patients with intractable pain, similar ideas have been formulated by Garcia-Larrea et al. (47,48). A CBF increase was found during MCS in the thalamus ipsilateral to stimulation, in the orbitofrontal and cingulate gyri, in the upper brainstem (49), and in the anterior insula/medial temporal lobe (50).** It was stated that these results highlight the thalamus as the key structure mediating functional MCS effects. Thalamic activation would trigger a cascade of synaptic events influencing activity in other pain-related structures, including the anterior cingulate gyrus, insula/medial temporal lobe, subthalamic areas, and the upper brainstem. As a consequence, MCS could influence the affective-emotional component of chronic pain by way of cingulate/orbitofrontal effects (51) and lead to descending inhibition of pain impulses by activation of the brainstem (47).

Effect of Stimulation Mode

When comparing stimulation in tonic mode to stimulation in burst mode, it was demonstrated that tonic mode stimulation generally yields more pronounced effects.

To our knowledge, there are no other studies comparing the central effects of burst and tonic stimulation mode of ONS. However, Sherman et al. (52) focused on the thalamus and found that all thalamic relay cells respond to excitatory inputs in one or both modes. The two firing modes strongly affect the manner by which thalamic relay cells respond to incoming inputs. They demonstrated that thalamic burst mode activated cortical cells more than tonic stimulation. These findings seem to conflict with our obtained data, but an explanation can be proposed when assessing the effect of frequency.

Effect of Frequency

When applying different stimulation frequencies in tonic mode, a larger MR-signal change was measured than when stimulating in burst mode. When performing a more in-depth analysis, it was shown that during tonic mode stimulation, all frequencies induced similar global activation or deactivation effects. In burst mode, on the contrary, the seven frequencies contribute differently to the global brain activity. These preliminary data show that there is a difference between harmonics of 3 Hz (3, 6, 12, and 18 Hz) and harmonics of 5 Hz (5, 10, and 20 Hz). The harmonics of 3 Hz (especially 3, 6, and 18 Hz) have the largest contribution to the global brain activity. Additionally, an intensity-effect can be seen in a few regions, such as the middle cingulate gyrus (Fig. 5d), PAG (Fig. 5f), S1 (Fig. 5g), V1 (Fig. 5h), and S2 (Fig. 5k). There appears to be a relation between the frequency and the percent MR-signal change, but the extent of this relation remains to be elucidated in future studies. Furthermore, questions remain concerning the differential effects seen when stimulating with harmonics of 3 Hz or 5 Hz. On one hand, it could be that different harmonics induce different physiologic effects, but on the other hand it could also be that the observation of such an effect is an accidental finding in this study. Therefore, further prospective study is needed to assess the effect of stimulation frequency to its full extent.

We are aware of the shortcomings of this experiment, namely the use of only one healthy volunteer, the limited number of stimulation frequencies, the lack of subthreshold stimulation, and the lack of blinding. However, this is a pioneer study, to provide on one hand insight in the feasibility of fMRI while stimulating the occipital nerves by means of externalized electrodes and on the other hand the central nervous system effects of ONS objectively visualized by means of 3T fMRI in a healthy volunteer. Therefore, this study is the starting point to numerous studies helping us to understand the working mechanism of neuromodulation techniques for the treatment of intractable pain.

CONCLUSION

As long as severe safety precautions are taken, it is feasible to perform 3T fMRI studies with simultaneous subcutaneous ONS. ONS seems to evoke distinct, but significant (de)activation patterns in the brain, in which tonic mode stimulation has an overall larger effect. This overall larger effect can partially be explained by an effect of used stimulation frequency. The unravelling of these patterns could contribute to the understanding of the beneficial effects seen in ONS treatment of patients with chronic pain.

Acknowledgments

We thank St. Jude Medical for their support.

Authorship Statements

The authors contributed in the following way: hypothesis and study design: D. DeRidder, S. Kovacs, S. Sunaert, T. Menovsky, and M. Plazier. Data collection: S. Kovacs and S. Sunaert. Experimental setup, safety testing and data analysis: R. Peeters and S. Kovacs. Manuscript draft preparation: S. Kovacs, D. DeRidder, M. Plazier, and T. Menovsky. Editorial support: T. Menovsky, D. DeRidder, and S. Sunaert. All authors approved the final manuscript.

How to Cite this Article:

Kovacs S., Peeters R., De Ridder D., Plazier M., Menovsky T., Sunaert S. 2010. Central Effects of Occipital Nerve Electrical Stimulation Studied by Functional Magnetic Resonance Imaging. *Neuromodulation* 2011; 14: 46–57

REFERENCES

- Tsubokawa T, Katayama Y, Yamamoto T, Hirayama T, Koyama S. Treatment of thalamic pain by chronic motor cortex stimulation. *Pacing Clin Electrophysiol* 1991;14:131–134.
- Green AL, Owen SL, Davies P, Moir L, Aziz TZ. Deep brain stimulation for neuropathic cephalgia. *Cephalalgia* 2006;26:561–567.
- Siegfried J. Sensory thalamic neurostimulation for chronic pain. *Pacing Clin Electrophysiol* 1987;10:209–212.
- Schoenen J, Di Clemente L, Vandenheede M et al. Hypothalamic stimulation in chronic cluster headache: a pilot study of efficacy and mode of action. *Brain* 2005;128:940–947.
- Osenbach R. Neurostimulation for the treatment of intractable facial pain. *Pain Medicine* 2006;7:5126–5136.
- Slavin KV, Nersesyan H, Wess C. Peripheral neurostimulation for treatment of intractable occipital neuralgia. *Neurosurgery* 2006;58:112–118.
- Weiner RL. Occipital neurostimulation (ONS) for treatment of intractable headache disorders. *Pain Med* 2006;7:5137–5139.
- Popeney CA, Aló KM. Peripheral neurostimulation for the treatment of chronic, disabling transformed migraine. *Headache* 2003;43:369–375.
- Bartsch T, Goadsby PJ. Stimulation of the greater occipital nerve induces increased central excitability of dural afferent input. *Brain* 2002;125:1496–1509.
- Le Doaré K, Akerman S, Holland PR et al. Occipital afferent activation of second order neurons in the trigeminocervical complex in rat. *Neurosci Lett* 2006;403:73–77.
- Goadsby PJ, Knight YE, Hoskin KL. Stimulation of the greater occipital nerve increases metabolic activity in the trigeminal nucleus caudalis and cervical dorsal horn of the cat. *Pain* 1997;73:23–28.
- Busch V, Frese A, Bartsch T. The trigemino-cervical complex. Integration of peripheral and central pain mechanisms in primary headache syndromes. *Schmerz* 2004;18:404–410.
- Busch V, Jakob W, Juergens T, Schulte-Mattler W, Kaube H, May A. Functional connectivity between trigeminal and occipital nerves revealed by occipital nerve blockade and nociceptive blink reflexes. *Cephalalgia* 2006;26:50–55.
- Ogawa S, Lee TM, Kay AR, Tank DW. Brain magnetic resonance imaging with contrast dependent on blood oxygenation. *Proc Natl Acad Sci USA* 1990;87:9868–9872.
- Bhidayasiri R, Bronstein JM, Sinha S et al. Bilateral neurostimulation systems used for deep brain stimulation: in vitro study of MRI-related heating at 1.5 T and implications for clinical imaging of the brain. *Magn Reson Imaging* 2005;23:549–555.
- Georgi JC, Stippich C, Tronnier VM, Heiland S. Active deep brain stimulation during MRI: a feasibility study. *Magn Reson Med* 2004;51:380–388.
- Rezai AR, Finelli D, Nyenhuis JA et al. Neurostimulation systems for deep brain stimulation: in vitro evaluation of magnetic resonance imaging-related heating at 1.5 tesla. *J Magn Reson Imaging* 2002;15:241–250.
- Shellock FG. Metallic neurosurgical implants: evaluation of magnetic field interactions, heating, and artifacts at 1.5-Tesla. *J Magn Reson Imaging* 2001;14:295–299.
- Kapural L, Mekhail N, Hayek SM, Stanton-Hicks M, Malak O. Occipital nerve electrical stimulation via the midline approach and subcutaneous surgical leads for treatment of severe occipital neuralgia: a pilot study. *Anesth Analg* 2005;101:171–174.
- Rorden C, Brett M. Stereotaxic display of brain lesions. *Behav Neurol* 2000;12:191–200.
- Tzourio-Mazoyer N, Landeau B, Papathanassiou D et al. Automated anatomical labeling of activations in SPM using a macroscopic anatomical parcellation of the MNI MRI single-subject brain. *Neuroimage* 2002;15:273–289.
- Shellock FG, Crues JV. MR procedures: biologic effects, safety, and patient care. *Radiology* 2004;232:635–652.
- Rezai AR, Phillips M, Baker KB et al. Neurostimulation system used for deep brain stimulation (DBS): MR safety issues and implications of failing to follow safety recommendations. *Invest Radiol* 2004;39:300–303.
- Henderson JM, Tkach J, Phillips M, Baker K, Shellock FG, Rezai AR. Permanent neurological deficit related to magnetic resonance imaging in a patient with implanted deep brain stimulation electrodes for Parkinson's disease: case report. *Neurosurgery* 2005;57:E1063.
- Spiegel J, Fuss G, Backens M et al. Transient dystonia following magnetic resonance imaging in a patient with deep brain stimulation electrodes for the treatment of Parkinson disease. Case report. *J Neurosurg* 2003;99:772–774.
- Finelli DA, Rezai AR, Ruggieri PM et al. MR imaging-related heating of deep brain stimulation electrodes: in vitro study. *Am J Neuroradiol* 2002;23:1795–1802.
- Rezai AR, Baker KB, Tkach JA et al. Is magnetic resonance imaging safe for patients with neurostimulation systems used for deep brain stimulation? *Neurosurgery* 2005;57:1056–1060.
- Rezai AR, Finelli D, Ruggieri P, Tkach J, Nyenhuis JA, Shellock FG. Neurostimulators: potential for excessive heating of deep brain stimulation electrodes during magnetic resonance imaging. *J Magn Reson Imaging* 2001;14:488–489.
- Baker KB, Tkach JA, Nyenhuis JA et al. Evaluation of specific absorption rate as a dosimeter of MRI-related implant heating. *J Magn Reson Imaging* 2004;20:315–320.
- Brodkey JS, Miyazaki Y, Ervin FR, Mark VH. Reversible heat lesions with radiofrequency current. A method of stereotactic localization. *J Neurosurg* 1964;21:49–53.
- Cosman ER Jr, Cosman ER Sr. Electric and thermal field effects in tissue around radiofrequency electrodes. *Pain Med* 2005;6:405–424.
- Houdas Y, Ring EF. *Temperature distribution. Human body temperature: its measurements and distribution*. New York: Plenum Publishing, 1982.
- Cosman ER. Radiofrequency lesions. In: Gildenberg PL, Tasker RR, eds. *Textbook of stereotactic and functional neurosurgery*. New York: McGraw Hill, 1998: 973–986.
- Deetjen P, Speckmann EJ. *Physiologie*. Munich: Urban-Fischer, 1999:19–20.
- Bruggencate G, Creutzfeldt O, Dudel J et al. *Allgemeine neurophysiologie*. Munich: Urban & Schwarzenberg, 1974:96.
- Matharu M, Bartsch T, Ward N, Frackowiak R, Weiner R, Goadsby P. Central neuro-modulation with implanted suboccipital stimulators in patients with chronic migraine. *Cephalalgia* 2003;23:655.
- Newman HM, Stevens RT, Apkarian AV. Direct spinal projections to limbic and striatal areas: anterograde transport studies from the upper cervical spinal cord and the cervical enlargement in squirrel monkey and rat. *J Comp Neurol* 1996;365:640–658.
- Burstein R, Potrebic S. Retrograde labeling of neurons in the spinal cord that project directly to the amygdala or the orbital cortex in the rat. *J Comp Neurol* 1993;335:469–485.
- Pfaller K, Arvidsson J. Central distribution of trigeminal and upper cervical primary afferents in the rat studied by anterograde transport of horseradish peroxidase conjugated to wheat germ agglutinin. *J Comp Neurol* 1988;268:91–108.
- Mouton LJ, Klop EM, Holstege G. C1-C3 spinal cord projections to periaqueductal gray and thalamus: a quantitative retrograde tracing study in cat. *Brain Res* 2005;1043:87–94.
- Keay KA, Bandler R. Anatomical evidence for segregated input from the upper cervical spinal cord to functionally distinct regions of the periaqueductal gray region of the cat. *Neurosci Lett* 1992;139:143–148.
- Carstens E, Trevino DL. Anatomical and physiological properties of ipsilaterally projecting spinothalamic neurons in the second cervical segment of the cat's spinal cord. *J Comp Neurol* 1978;182:167–184.
- Matsushita M, Xiong G. Uncrossed and crossed projections from the upper cervical spinal cord to the cerebellar nuclei in the rat, studied by anterograde axonal tracing. *J Comp Neurol* 2001;432:101–118.
- Yingling CD, Skinner JE. Selective regulation of thalamic sensory relay nuclei by nucleus reticularis thalami. *Electroencephalograph. Clin Neurophysiol* 1976;41:476–482.
- Peyron R, Laurent B, Garcia-Larrea L. Functional imaging of brain responses to pain. A review and meta-analysis (2000). *Neurophysiol Clin* 2000;30:263–288.
- May A. A review of diagnostic and functional imaging in headache. *J Headache Pain* 2006;7(4):174–184.
- Garcia-Larrea L, Peyron R, Mertens P, Laurent B, Maugeiere F, Sindou M. Functional imaging and neurophysiological assessment of spinal and brain therapeutic modulation in humans. *Arch Med Res* 2000;31:248–257.
- Garcia-Larrea L, Peyron R, Mertens P et al. Electrical stimulation of motor cortex for pain control: a combined PET-scan and electrophysiological study. *Pain* 1999;83:259–273.
- Peyron R, Garcia-Larrea L, Deiber MP et al. Electrical stimulation of precentral cortical area in the treatment of central pain: electrophysiological and PET study. *Pain* 1995;62:275–286.
- Garcia-Larrea L, Peyron R, Laurent B, Maugeiere F. Association and dissociation between laser-evoked potentials and pain perception. *Neuroreport* 1997;8:3785–3789.
- Dostrovsky JO, Hutchinson WD, Davis KD, Lazano A. Potential role of orbital and cingulate cortices in nociception. In: Besson JM, Guilbaud G, Ollat H, eds. *Forebrain areas involved in pain processing*. Paris: John Libbey Eurotext, 1995: 171–181.
- Sherman SM. Tonic and burst firing: dual modes of thalamocortical relay. *Trends Neurosci* 2001;24:122–126.

COMMENTS

This is a very important study that may become a beginning of new era of clinical research. Peripheral nerve stimulation (and particularly occipital nerve stimulation) rapidly becomes widely accepted by the neuromodulation community as the means of pain control in various clinical circumstances. At the same time, the lack of basic understanding on how it all works raises many concerns regarding its applicability, safety, long-term effects, patient selection and many other areas related to this attractive and minimally-invasive modality.

In the past, MRI incompatibility of existent neurostimulation devices precluded investigators from using MRI as a research tool—hence the previous experience with PET studies investigating effects of ONS on brain activity,¹ cited by the authors. Functional MRI, however, provides better spatial and temporal resolution, and its use in defining central effects of ONS/PNS is highly desirable. Therefore, appearance of this research paper is very timely. I applaud the authors in developing the protocol, following minute details and securing a volunteer for the project.

To some extent, this resembles initial pioneering experience of famous neurosurgeons and neuroscientists of the past—when Drs. Patrick D. Wall and William H. Sweet inserted PNS electrodes into their own infraorbital foramina in order to show pain suppression during electrical nerve stimulation and thereby provide some proof of the “gate-control” theory of pain.²

I agree with the authors that their conclusions, based on a single person without chronic pain, should not be taken as an ultimate explanation of observed clinical effects of ONS. Eventually, we may find that central processing changes in response to chronic suffering and varies in different clinical conditions (such as migraines, cluster headaches, occipital neuralgia, fibromyalgia—just to name few diagnoses for which this modality has been successfully used), and therefore ONS may have different effects in different patient populations.

Development of MRI-compatible neurostimulation devices may eliminate our concerns about safety of MRI-based research projects. But until these devices are available, we will have to rely on dedication of those few research centers that are equipped with expertise to define safe scanning procedures and are willing to pursue in-depth investigation of cerebral neuromodulation processes.

In my opinion, this paper creates more questions than answers—and to address them all, the authors and other researchers will have to continue developing research paradigms in exploring the mechanisms that underlie our clinical observations. One has to keep in mind, however, that data described in this paper does not provide blanket safety statement regarding high-power MRI in ONS and, in particular, does not address the issue of MRI safety in patients with implanted neurostimulation generators.

Konstantin V. Slavin, MD
Professor
Neurological Surgery—CS
University of Illinois at Chicago
Chicago, IL, USA

References:

1. Matharu MS, Bartsch T, Ward N, Frackowiak RS, Weiner R, Goadsby PJ. Central neuromodulation in chronic migraine patients with suboccipital stimulators: a PET study. *Brain* 2004;127:220–230.
2. Wall PD, Sweet WH. Temporary abolition of pain in man. *Science* 1967;155:108–109, Konstantin Slavin, MD.

I congratulate the authors on presenting a cogent and very informative, detailed analysis of an ONS neurophysiologic response using state of the art fMRI technology. This initial study not only helps correlate peripheral nervous system influences on central processes and responses, but also shows that MRI technologies can be used safely to further our understanding of CNS/PNS neurostimulation mechanisms.

Richard Weiner, MD
Dallas Neurosurgical Associates
Dallas, TX, USA

In “Central Effects of Occipital Nerve Stimulation Studied By fMRI”¹⁰ Kovacs et al. provide a valuable proof-of-concept study of a single patient in whom the patterns of cortical activation induced by tonic or burst mode occipital nerve stimulation were examined with fMRI. Importantly, they describe their study-specific phantom preparation, as issues related to MRI safety in studies of implanted electrodes are highly dependent on the details of electrode composition, orientation and position, as well as of the scan parameters, including SAR and frequencies. Significant attention has been turned to MRI safety with implanted neurostimulators, but most of this work has been done in reference to deep brain stimulation^{1–3,6,8,9} or electrodes in the spinal canal.^{4,9} This article draws important attention to the fact that many of these concerns are not as severe in PNS implantations as in the brain or over the spinal cord.

It is interesting that they appear to have implanted a normal volunteer. At many centers, there would be considerable concern about performing an invasive procedure to manipulate cerebral metabolism, without a clinical indication, as a safety study. The results are very general, as expected. As in studies of SCS⁵ and VNS,⁷ the patterns of activation and deactivation are quite broad and difficult to interpret in a single study without an a priori hypothesis in question. The differential response to bursting versus tonic stimulation is particularly inviting for further investigation.

Kenneth M. Aló, MD
Director, Interventional Pain Medicine
Houston Texas Pain Management
Houston, TX, USA
Associate Professor and NeuroCardiology Section Director
Institute of Cardiology and Vascular Medicine
Monterrey Technical University
Monterrey, Mexico
Erich Richter, MD
Assistant Professor of Neurosurgery
Department of Neurosurgery
LSU Health Sciences Center
New Orleans, LA, USA

References

1. Arantes PR, Cardoso EF, Barreiros MA, Teixeira MJ, Goncalves MR, Barbosa ER, Sukwinder SS, Leite CC, Amaro E, Jr. Performing functional magnetic resonance imaging in patients with Parkinson’s disease treated with deep brain stimulation. *Mov Disord* 2006;21:1154–1162.
2. Baker KB, Tkach J, Hall JD, Nyenhuis JA, Shellock FG, Rezaei AR. Reduction of magnetic resonance imaging-related heating in deep brain stimulation leads using a lead management device. *Neurosurgery* 2005;57:392–397; discussion 392–397.
3. Chhabra V, Sung E, Mewes K, Bakay RA, Abosch A, Gross RE. Safety of magnetic resonance imaging of deep brain stimulator systems: a serial imaging and clinical retrospective study. *J Neurosurg* 2009.
4. De Andres J, Valia JC, Cerda-Olmedo G, Quiroz C, Villanueva V, Martinez-Sanjuan V, de Leon-Casasola O. Magnetic resonance imaging in patients with spinal neurostimulation systems. *Anesthesiology* 2007;106:779–786.

5. Kiriakopoulos ET, Tasker RR, Nicosia S, Wood ML, Mikulis DJ. Functional magnetic resonance imaging: a potential tool for the evaluation of spinal cord stimulation: technical case report. *Neurosurgery* 1997;41:501–504.
6. Larson PS, Richardson RM, Starr PA, Martin AJ. Magnetic resonance imaging of implanted deep brain stimulators: experience in a large series. *Stereotact Funct Neurosurg* 2008;86:92–100.
7. Liu WC, Mosier K, Kalnin AJ, Marks D. BOLD fMRI activation induced by vagus nerve stimulation in seizure patients. *J Neural Neurosurg Psychiatry* 2003;74:811–813.
8. Tagliati M, Jankovic J, Pagan F, Susatia F, Isaias IU, Okun MS. Safety of MRI in patients with implanted deep brain stimulation devices. *Neuroimage* 2009;47(Suppl 2):T53–57.
9. Tronnier VM, Staubert A, Hahnel S, Sarem-Aslani A. Magnetic resonance imaging with implanted neurostimulators: an in vitro and in vivo study. *Neurosurgery* 1999;44:118–125; discussion 125–116.
10. Kovacs S, Peeters R, DeRidder D, Plazier M, Menovsky T, Sunaert S. (in press). Central effects of occipital nerve electrical stimulation studied by fMRI. *Neuromodulation: Technology at the Neural Interface*.

Comments not included in the Early View version of this paper.